Title

Ancient European dog genomes reveal continuity since the Early Neolithic

Authors

Laura R. Botigué[1,†], Shiya Song[2,†], Amelie Scheu[3,8,†], Shyamalika Gopalan[1], Amanda L. Pendleton[4], Matthew Oetjens[4], Angela M. Taravella[4], Timo Seregély[5], Andrea Zeeb-Lanz[6], Rose-Marie Arbogast[7], Dean Bobo[1], Kevin Daly[8], Martina Unterländer[3], Joachim Burger[3], Jeffrey M. Kidd[2,4], Krishna R. Veeramah[1,*]

Affiliations

[1] Department of Ecology and Evolution, Stony Brook University, Stony Brook, New York, 11794-5245, USA.

[2] Department of Computational Medicine and Bioinformatics, University of Michigan, Ann Arbor, MI 48109, USA.

[3] Palaeogenetics Group, Johannes Gutenberg-University Mainz, 55099 Mainz, Germany.

[4] Department of Human Genetics, University of Michigan, Ann Arbor, MI 48109, USA.

[5] Department of Prehistoric Archaeology, Institute of Archaeology, Heritage Sciences and Art History, University of Bamberg, 96045 Bamberg, Germany.

[6] Generaldirektion Kulturelles Erbe Rheinland-Pfalz, State Archaeology, Department for Monumental Heritage Speyer, 67346 Speyer, Germany.

[7] CNRS UMR 7044-UDS, 5 allée du Général Rouvillois F 67083 Strasbourg, France.

[8] Smurfit Institute of Genetics, Trinity College Dublin, Dublin 2, Ireland.

†These authors contributed equally to this work

*corresponding author: krishna.veeramah@stonybrook.edu

Keywords

Ancient DNA, dog domestication, Neolithic, Europe

Abstract

Europe has played a major role in dog evolution, harbouring the oldest uncontested Paleolithic remains and having been the centre of modern dog breed creation. We sequenced the whole genomes of an Early and End Neolithic dog from Germany, including a sample associated with one of Europe's earliest farming communities. Both dogs demonstrate continuity with each other and predominantly share ancestry with modern European dogs, contradicting a previously suggested Late Neolithic population replacement. Furthermore, we find no genetic evidence to support the recent hypothesis proposing dual origins of dog domestication. By calibrating the mutation rate using our oldest dog, we narrow the timing of dog domestication to 20,000-40,000 years ago. Interestingly, we do not observe the extreme copy number expansion of the *AMY2B* gene that is characteristic of modern dogs and has previously been proposed as an adaptation to a starch-rich diet driven by the widespread adoption of agriculture in the Neolithic.

Europe has been a critically important region in the history and evolution of dogs, with most modern breeds sharing predominantly European ancestry [1]. Furthermore, the oldest remains that can be unequivocally attributed to domestic dogs (*Canis lupus familiaris*) are found on this continent, including an Upper Paleolithic 14,700-year-old jaw-bone from the Bonn-Oberkassel site in Germany [2]; although older specimens from Siberia and the Near East have been proposed, these are highly controversial [3,4]. Analysis of mitochondrial and genomic data from modern dogs have suggested East Asia [5,6], the Middle East [7] and Central Asia [8] all as potential centers of dog domestication. However, ancient mitochondrial DNA (mtDNA) suggests a European origin [9].

The Neolithic period in Central Europe ranges from ~7,500-4,000 BP and can be further subdivided based on specific features of human culture (Supplementary Methods 1). Intriguingly, multiple studies have found evidence of a striking prehistoric turnover of canid mtDNA lineages in the European continent sometime between the Late Neolithic and today, with haplogroup C, which appears in almost all Neolithic dogs but in less than 10% of modern dogs, being replaced by haplogroup A in most of Europe [9–11]. By analyzing genomic data from modern dogs as well as a Late Neolithic (~5,000 years old) Irish dog from Newgrange (hereafter referred to as NGD), Frantz et al. [11] argue that this matrilineal turnover was a consequence of a major population replacement. However, NGD primarily shares ancestry with modern European dogs, implying the proposed population replacement had largely already occurred before this

individual lived. Frantz et al. also estimate a relatively recent east-west dog divergence (14,000-6,000 years ago), which, placed within the context of existing archaeological data, they explain with a dual origin hypothesis.

The characterization of samples from earlier in the Neolithic and from continental Europe are therefore necessary to examine whether and to what extent a large-scale demographic replacement occurred in Europe during this period. This would be evidenced by a distinct ancestry absent in modern dog genomes that was more prominent in dogs from earlier in the Neolithic, as opposed to genomic continuity from the Early Neolithic to today. This, in turn, is key for understanding human-dog interactions during the major replacement of indigenous Paleolithic hunter-gatherers by Neolithic farmers from Anatolia [12,13] and the subsequent migrations from the Eastern European steppe [14], as well as for disentangling the process of dog domestication.

We present analysis of ~9x coverage whole genomes of two dog samples from Germany dating to the Early and End Neolithic (~7,000 years old and ~4,700 years old, respectively; Supplementary Methods 1-4). We observe genetic continuity throughout this era and into the present, with our ancient dogs sharing substantial ancestry with modern European dogs, and our Early Neolithic dog being almost indistinguishable from NGD. We find no evidence of a major population replacement; instead, our results are consistent with a scenario where modern European dogs emerged from a structured Neolithic population, consistent with the previously reported turnover in mitochondrial haplogroups. Furthermore, we detect an additional ancestry component in the End Neolithic sample, consistent with admixture from a population of dogs located further east that may have migrated concomitant with steppe people associated with Late Neolithic and Early Bronze age cultures, such as the Yamnaya and Corded Ware. We also show that most autosomal haplotypes associated with domestication were already established in our Neolithic dogs, but that adaptation to a starch-rich diet likely occurred later. We obtain divergence estimates between Eastern and Western dogs of 17,000-24,000 years ago, compatible with the archaeological record and consistent with a single geographic origin for domestication, the timing of which we narrow down to between ~20,000-40,000 years ago.

Results

Archaeological samples and ancient DNA sequencing

The older specimen (and the oldest whole nuclear dog genome sequenced to date), which we refer to hereafter as HXH, was found at the Early Neolithic site of Herxheim and is dated to 5,223-5,040 cal. BCE (~7,000 years old) (Supplementary Figure S1.2.1). The younger specimen, which we refer to hereafter as CTC, was found in Kirschbaumhöhle (Cherry Tree Cave) and is dated to 2,900-2,632 cal. BCE (~4,700 years old), which corresponds to the End Neolithic period in Central Europe [15] (Supplementary Figure S1.3.1).

We generated paired-end Illumina whole-genome sequencing data for the two ancient dog samples and successfully mapped over 67% of the reads to the dog reference genome (CanFam3.1), confirming high endogenous canine DNA content for both samples (Supplementary Methods 4). MapDamage [16] analysis demonstrated that both samples possessed characteristics typical of ancient DNA [17] such as a high frequency of 5' C>T and 3' G>A changes at the end of fragments (~35% and 28% of each transition category for HXH and CTC, respectively), while fragment length was also small (mean 60-70bp) (Supplementary Figure S4.1.1). Overall, we conclude that both our samples appear to contain substantial authentic canine ancient DNA. The final mean coverage for both samples was ~9x. Additionally, the mean coverage for the X and Y chromosomes was ~5x for both samples, indicating that both are males. We also reprocessed the NGD data [11] using the same pipeline and reference genome as for CTC and HXH. To call variants we used a custom genotype caller implemented in Python (see Supplementary Methods 5) that accounts for DNA damage patterns estimated from MapDamage using the likelihood model described in [13]. We found that this method and the application of additional filters eliminated many false positives that are likely due to postmortem damage (Supplementary Figure S5.1.2).

Modern Canid Reference Datasets

In order to better understand how these Neolithic dogs are genetically related to modern dogs, we analyzed them within the context of a comprehensive collection of 5,649 canids, including breed dogs, village dogs and wolves that had been previously genotyped at 128,743 SNPs [8,18], as well as 99 canid whole genomes sequenced at medium to high coverage (6-45x), including NGD.

In order to utilize whole genome data with such variable coverage (including our ancient samples), it is important that variable sites are chosen in a manner that will not bias downstream population genetic analysis. One popular approach exemplified by the *f-statistic* analyses of

Patterson et al. [19] is to ascertain variable sites in an outgroup (i.e. such that mutations are known to have occurred in the root of all the populations being analyzed). We thus explored different ascertainment schemes for the whole genome data (Supplementary Methods 6.2). In each case, variant sites on the autosomes were identified in specific sets of individuals and then genotyped across all sequenced samples. For the SNP-based analysis of whole genomes presented below we chose to use a call set that only includes sites discovered as variable in New World wolves, though we note our primary results are robust to changes in the ascertainment scheme. This call set contains 1,815,911 variants which must either be private to New World wolves or arose in the gray wolf (*Canis lupus*) ancestral population, and thus is the least biased with regard to their ascertainment in Old World wolves and dogs. We note that gene flow between New World wolves and Old World canids could potentially bias the observed genetic variation in this call set. However, previous genomic studies have reported very low to negligible migration rates only between Mexican wolves and basenji/dingo [20] and analysis of one locus under positive selection that confers black coat color suggests a potential old introgression from dogs to North American wolves (though we note that selection on standing variation cannot be ruled out) [21]. In both cases, these admixture events should have minimal impact on our analyses which primarily involve Eurasian dogs.

Mitochondrial DNA analysis

We examined the phylogenetic relationship of the entire mitochondrial genomes of HXH and CTC with a comprehensive panel of modern dogs across four major clades (A-D), modern wolves and coyotes, and previously reported [9,11] ancient wolf-like and dog-like whole mitochondrial sequences. Like other European Neolithic dogs, both HXH and CTC belong to haplogroup C (Figure 1a and Supplementary Methods 7), together with NGD and the Upper Paleolithic 12,500 year old Kartstein Cave dog (also from Germany). We note that Bonn-Oberkassel also falls in the same haplogroup [9], although analysis of this sample is complicated by low mtDNA sequence coverage (see Supplementary Methods 7), pointing to some degree of matrilineal continuity in Europe over ~10,000 years, ranging from the Late Paleolithic to almost the entire Neolithic. The inclusion of 24 additional clade C samples [22] in the phylogenetic analysis reveals the expected C1 and C2 split (100% support) and that HXH, CTC, NGD and the ancient German dog share a common lineage with C1 dogs (Supplementary Figure S7.2.2). This topology suggests that these ancient European dogs belong to an older, novel sub-haplogroup that is sister to the progenitor of the C1b and C1a sub-haplogroups and possibly absent in modern dog populations. Incorporation of additional whole mtDNA sequences from

both ancient and modern dogs will determine whether this sub-haplogroup lineage has gone extinct in Europe or is simply missing from our current sample set.

Genomic clustering of the European Neolithic dogs

We constructed a neighbor-joining (NJ) tree using the whole genome sequence dataset (Figure 1b) to determine which modern dog population shows the greatest genetic similarity to the ancient samples. We found that the Early Neolithic HXH and Late Neolithic NGD grouped together as a sister clade to modern European village dogs, while CTC was external to this clade, but still more similar to it than any other modern canid population. As shown previously [11], East Asian village dogs and breeds are basal to all other dogs.

We also performed a PCA using both the SNP array and whole genome data (Figure 2a, 2b and Supplementary Methods 8), with both datasets showing essentially the same pattern of population structure, despite having very different ascertainment schemes (SNP array data is expected to be biased towards European breed dogs). The larger SNP array reference dataset shows that village dogs primarily separate into five distinct geographic clusters: Southeast Asia (Vietnam, Indonesia, Thailand, China), India, Middle East (Lebanon, Qatar, Turkey, Saudi Arabia, Armenia, Iraq), Europe, and Africa. Breed dogs fall mostly within European village dogs' variation with the exception of basal or "ancient" breeds [23], which are located within the axis of their geographical origin. Consistent with NJ tree analysis, all three ancient samples fell within the range of modern dog variation. HXH and NGD are the ancient samples found closest to the major European cluster, both lying adjacent to the cluster of Pacific Island dogs that are thought to be derived almost completely from European dogs [8]. CTC is located next to village dogs from Afghanistan, a known admixed population also inferred to have a major European-like ancestry component, as well as potential contributions from South and East Asian populations [8].

We note that the position of NGD in our reanalysis does not agree with that reported in Frantz et al. [11], where it lies as an outlier in PC2. Such deviation was interpreted by Frantz et al. as NGD carrying ancestry from an extinct European population. However, we found that the isolated position of NGD is entirely due to a technical artifact that occurred by the inclusion of both the uncalibrated and calibrated ancient genome samples in the same PCA. Once one of the duplicate NGD data points is removed from the sample set, this individual moves back to the general modern dog cluster (Supplementary Methods 15). We also note fundamental differences in the overall distribution of genetic variance in PC space in both studies due to the

overall ascertainment of samples. Since our dataset contains a substantially more diverse collection of samples, which includes various breeds and globally distributed village dogs, we assert that our PCA results are more reflective of the true range of dog diversity.

We further examined the genetic relatedness between ancient and modern dogs by performing an $f3$-outgroup analysis on both the SNP array and whole genome sequence datasets. This method has been used previously in ancient DNA studies to investigate how modern populations are genetically related to an ancient sample [13,24–26]. Assuming a simple three population model with no post-divergence gene flow, where population C is an outgroup to A and B, the value of this statistic will reflect the amount of shared drift between A and B relative to C. We used the golden jackal and Andean fox as outgroups for both the SNP array and the whole genome datasets, respectively. If one population (e.g. B) is kept constant, in this case an ancient dog, then introducing different populations to represent A will provide relative estimates of genetic similarity with B (note this makes no assumptions with regard to the complexity of the demographic history that connects populations A and B). Our results corroborated NJ tree and PCA findings, and showed that all three Neolithic European samples share most of their ancestry with modern dogs from Europe (Figure 3 and Supplementary Figures S10.1.1-2; Supplementary Methods 10).

Evidence of admixture in Neolithic dogs

Our results are consistent with continuity of a European-like genetic ancestry from modern dogs through the entire Neolithic period, and, based on mtDNA from Bonn-Oberkassel, perhaps even into the Upper Paleolithic. However, the slightly displaced position of the ancient samples from the European cluster in the PCAs (particularly for CTC) suggests a complex history possibly involving ancestry from other sources. We therefore performed unsupervised clustering analyses with ADMIXTURE (SNP array data; Supplementary Figure S8.3.2) and NGSadmix (whole genome data; Figure 4 and Supplementary Figure S8.4.1) (Supplementary Methods 8) and found that, unlike contemporary European village dogs, all three ancient genomes possess a significant ancestry component that is present in modern Southeast Asian dogs. This component appears only in a minority of modern European village dogs at very low levels. Furthermore, CTC harbors an additional component that is found predominantly in modern Indian village as well as in Central Asian (Afghan, Mongolian and Nepalese), and Middle Eastern (Saudi Arabian and Qatari) dogs, concordant with its position in the PCA, as well as some wolf admixture.

We formally modelled these potential admixture events by applying the tree-based framework, MixMapper [27] to both the SNP array and whole genome data. This approach interrogates every pair of branches in a scaffold tree to infer putative sources of admixture for non-scaffold target samples (in this case HXH, CTC and NGD) via the fitting of *f-statistics* observed in the data. We constructed the scaffold tree excluding those populations that showed evidence of admixture as determined by an *f3* statistic test (see Supplementary Methods 10). MixMapper inferred that HXH and NGD were both formed by an admixture event involving the ancestors of modern European and Southeast Asian dogs. An *f4*-ratio test estimated ~19-30% Southeast Asian-like gene flow into HXH and NGD (Supplementary Methods 10). Analysis with ADMIXTUREGRAPH [28] on the whole genome data, a method related to MixMapper that examines a manually defined demographic history, demonstrated a perfect fit for the observed *f-statistics* under this model (Supplementary Methods 11).

In order to disentangle the more complex admixture patterns observed in CTC, we first sought to understand its relationship to HXH given that both samples originate from Germany. Interestingly, we found an indication of possible genetic continuity between both samples with our *f3*-outgroup analysis, which revealed that CTC had greater affinity with HXH (followed by other European populations) than with any modern canid or with NGD (Figure 3b and Supplementary Figure S10.1.1-2; Supplementary Methods 10). We therefore performed a MixMapper analysis where HXH was set as one of the sources of admixture for CTC, which identified a population ancestral to modern Indian or Saudi Arabian village dogs as the second source of admixture, supporting the pattern identified in the unsupervised clustering analyses.

However, given that HXH and modern European dogs share substantial genetic ancestry, it is possible that the observed European-like component in CTC is derived from a different lineage than HXH (for example, via a distinct Eurasian admixed population that migrated into Germany sometime during the Neolithic). To test this, we used ADMIXTUREGRAPH to compare a model of canid demography where a) CTC descended from the same population as HXH followed by admixture with an Indian-like population versus b) both ancient samples being descended from independently diverged European lineages. The model with CTC as a descendant of HXH (Figure 5a) provides a much better fit to the data. This scenario produced only two *f4* outliers (no *f2* or *f3* outliers), one of which was barely significant (Z=3.013), whereas a model where the two ancient samples are descended from different ancestral European populations produced 74 outliers (Supplementary Methods 11). Even though there is the risk of overfitting the model to

the data, the stark difference in the fit of the two models point to general continuity amongst German dogs during the Neolithic, along with admixture towards the latter end of this era with an outside source carrying the genetic component shared with contemporary Middle Eastern and Central and South Asian dog populations. We also note that building a demographic model with ADMIXTUREGRAPH that fits the complex history found in CTC was extremely challenging (see Supplementary Methods 11).

We further investigated the wolf admixture inferred by the unsupervised clustering analysis with SpaceMix [29], a method similar to PCA that additionally incorporates the geographic location of the populations to create a "geogenetic" map (Supplementary Methods 8). It then detects deviations of increased covariance in this geogenetic space that are likely to reflect long-distance admixture events. The clustering of modern and ancient dogs in SpaceMix is essentially the same as observed in the PCA, with HXH and NGD closest to Pacific Island dogs and CTC found near Afghanistan dogs. However, SpaceMix additionally inferred around 10% ancestry in CTC (but not HXH or NGD) from the geogenetic space containing Old World wolves (Supplementary Figure S8.2.3). *f4* statistics of the form *f4*(CTC,HXH,Wolf,Outgroup) suggest that the likely origin of this wolf component is related to contemporary Iranian/Indian wolves (those with the least amount of dog admixture, as revealed using an *f4*-ratio test and SpaceMix; Supplementary Methods 10). In light of these results, and considering that in our sample set modern Indian dogs show the largest proportion of the ancestry detected in CTC, it is likely that an ancestral dog population carrying both this Asian dog and wolf ancestry admixed with the population represented by CTC. We find strong support for this scenario with ADMIXTUREGRAPH, where a model for CTC incorporating modern village dogs and wolves produces no outliers when we allow for an admixture event between European and Indian village dog lineages along with previous wolf gene flow into the Indian lineage (Supplementary Figure S11.2.1; Supplementary Methods 11).

The complex pattern of admixture found in CTC is similar to that observed in many modern dog populations in Central Asia (such as Afghanistan) and the Middle East, as shown in our unsupervised clustering analyses (Supplementary Figure S8.3.2). This raises the question of whether CTC and these modern dog populations share a common admixture history and are descended from the same ancestral populations. We performed a MixMapper analysis that included HXH in the scaffold tree and observed that the European-like component of CTC is drawn exclusively from this Early Neolithic German dog population, a finding consistent with our

ADMIXTUREGRAPH results. To the contrary, modern Afghan dogs generally demonstrate inferred ancestry from modern European village dogs. This suggests that modern Afghan village dogs and CTC are the result of independent admixture events, which in turn implies that dog gene flow across Eurasia has been occurring for thousands of years.

Demographic model and divergence time

The distinct genetic makeup of the European Neolithic dogs compared to modern European dogs indicates that while ancient and contemporary populations share substantial genomic ancestry, some degree of population structure was present on the continent. Neolithic dogs would thus represent a now extinct branch that is somewhat diverged from the modern European clade. In addition, our best fit model of modern and ancient canid demography using ADMIXTUREGRAPH involved a topology that would be consistent with a single dog lineage diverging from wolves (Figure 5a). Therefore, we attempted to infer the divergence time of HXH and NGD from modern European dogs after the divergence of the Indian lineage that, according to the NJ tree analysis, is the sister clade of the Western Eurasian branch. We note that this is a simplistic bifurcating model of what may have been more complex European geographic structuring and long term Eurasian dog gene flow.

We first used the coalescent-based G-PhoCS [30] analysis of the model in Figure 5b to obtain estimates of divergence time and population diversity. Analysis was performed on sequence data from 16,434 previously identified 1kb-long loci [31]. Unlike the SNP-based analysis described above, single-sample genotype calling was performed with no particular ascertainment scheme, and we restricted our analysis to eight canid genomes with coverage ranging from 8 to 24x. When we included only modern dogs, we observed that different modern wolf populations appeared to diverge rapidly, concordant with previous studies [20,31], whereas the branching of the main dog lineages took place over a much longer period of time. We found that the (uncalibrated) dog-wolf divergence time in units of expected numbers of mutations per site (0.5247×10^{-4}) was similar to that reported in Freedman [31]; however, our dog divergence time (0.2786×10^{-4}) was younger than the Freedman et al. [31] estimate, but similar to the Wang et al. [6] estimate, most likely as a result of using Southeast Asian village dogs rather than the dingo. We also found that the effective population size of village dogs was 5-10 fold higher than that of the boxer.

However, once the ancient samples were included in the G-PhoCS analysis, all divergence times increased markedly (except the boxer-European village dog split). Additionally, we detected an excess of private variants in the ancient samples (even for NGD, which was at high coverage) compared to European village dogs. It is likely that these results are due to remnant postmortem damage artificially inflating variation in the ancient samples and elongating the branch lengths in the G-PhoCS analysis. Therefore, we devised a new method for estimating the HXH-European split time, τ_1 (again, in units of expected numbers of mutations), that utilized G-PhoCS results for only the modern samples and would be robust to biases resulting from the use of ancient samples (Supplementary Methods 13 and Supplementary Figure S13.2.1). Specifically, we calculated the relative observed amount of derived allele sharing exclusive to European village dogs and HXH/NGD versus that exclusive to European and Indian village dogs. The two major advantages of this estimate are that a) it only depends on previously discovered variable sites in other higher coverage modern dogs (i.e. our genotype calling in ancient samples is likely to be much more accurate in such situations), and b) it uses only a single chromosome from each population (which can be randomly picked), and thus does not require calling heterozygotes accurately (i.e. it should not be sensitive to the lower coverage of our ancient samples). We then calculated the expectation of this ratio using coalescent theory (see Methods) and iterated over possible τ_1 values until the expectation of the ratio fell into the observed confidence interval. As expected considering the tree topology, European dogs share more derived alleles with the ancient dogs than Indian village dogs, with ratios of 1.186-1.217 for HXH and 1.195-1.231 for NGD. Our expectation was conditioned on the following parameter estimates from G-PhoCs: N_e for European/Boxer ancestral population (θ_1), N_e for European/Indian ancestral population (θ_2), time of divergence for Europe and Boxer (τ_0), time of divergence for Europe/India (τ_2) and time of divergence for Europe-India/Asia (τ_3), as well as the percentage of HXH that is made up of Asian admixture (α) from the *f4*-ratio analysis.

While our estimates of divergence times are in units of expected numbers of mutations, we can use the age of our ancient samples to calibrate the resulting divergence time in years. Specifically, we used the age of the HXH sample to set an upper bound for the yearly mutation rate μ, as the sample must be younger than the time in years since divergence of HXH and modern European dogs. Given that the sample is 7,000 years old, we infer that an upper bound for μ is 5.6×10^{-9} per generation (assuming a 3 year generation time, with a 95% CI for the upper bound of 3.7×10^{-9} to 7.4×10^{-9}, Supplementary Figure S13.5.1.c). This upper bound, which represents the highest mutation rate potentially compatible with the age of our samples, is

consistent with the rate of μ=4 x 10^{-9} per generation suggested by both Skoglund et al. [32] and Frantz et al. [11], two rates also calibrated by ancient samples. In contrast, a mutation rate of 6.6 x10^{-9}, based on phylogenetic analyses [33,34], would be coincident with our estimate of the upper bound and is not compatible with Skoglund et al. or Frantz et al. When we calibrate τ_1 using the slower mutation rate of μ=4 x 10^{-9} , we estimate a value of ~6,500-12,900 years for HXH and ~6,400-12,600 years for NGD. From the G-PhoCS analysis, we further estimated that modern European and Indian village dogs diverged ~13,700-17,900 years ago, both of which diverged from Southeast Asian dogs ~17,500-23,900 years ago as a basal dog divergence event. Finally, we estimated the dog-wolf divergence time to be 36,900-41,500 years ago (Figure 5b). We note that, though in line with previous studies [31,35], our estimates of east-west dog divergence are much older than those reported in Frantz et al. While we use a Bayesian approach with G-PhoCS to infer divergence times, Frantz et al. rely on an MSMC approach, the performance of which is strongly dependent on the accuracy of genomic phasing [36].

Functional variants associated with the domestication process

As a result of domestication from wolves, specific portions of dog genomes have significantly differentiated from their wild relatives [37]. To determine the domestication status of the three Neolithic dogs, we assessed haplotype diversity at candidate domestication loci. Using only breed dogs and wolves, a previous study identified thirty-six candidate domestication loci [37]. However, our analysis of a more diverse sample set that includes village dogs confirms only eighteen of these loci as putative domestication targets, while the remainder are likely associated with breed formation (Supplementary Methods 14). HXH appeared homozygous for the dog-like haplotype at all but one of these 18 loci, and thus was often indistinguishable from most modern dogs. The younger NGD appeared dog-like at all but two loci. CTC, however, was heterozygous for the wolf-like haplotype at six loci, compatible with its increased wolf ancestry described above (Supplementary Figure S8.2.3. and Supplementary Methods 8).

The Neolithic saw drastic changes in human culture and behavior, including the advent of agriculture, resulting in a shift toward more starch-rich diets. Elevated *AMY2B* copy-number, which is associated with increased efficiency of starch metabolism, has often been suggested to be a strong candidate feature of domestication, even though *AMY2B* copy-number is known to vary widely in diverse collections of modern wolves and breed dogs [31,38,39]. Although the dog haplotype is present in all three Neolithic samples at this locus (Figure 6a), none showed evidence for the extreme copy number expansion of *AMY2B* (Figure 6b). Based on read depth,

we estimate that CTC and HXH carried two copies of the *AMY2B* gene while NGD carried three copies, not two as previously reported [11] (Supplementary Methods 14). Analysis of the full sample set of canines shows a bimodal distribution of copy number, with most modern dogs having >6 *AMY2B* copies, while few carry 2 or 3 copies [39]. This dynamic and extreme copy-number increase is presumed to be the result of a tandem expansion of the AMY2B gene [37]. Further analysis of NGD read-depth profiles has revealed the presence of a larger, ~2 megabase segmental duplication encompassing the *AMY2B* gene locus on chromosome 6 and extending proximally toward the centromere. This duplication is present in eleven of the analyzed modern dog samples and appears to be independent of the extreme copy number expansion of the *AMY2B* gene itself (Supplementary Methods 14).

Discussion

The sequencing and analysis of two German Neolithic dog samples, and the reanalysis of a third Irish Neolithic sample, provides several new insights into the history of dog domestication. We find strong evidence for genetic continuity from the Paleolithic into the Neolithic, and, to some extent, the present. We do not find any evidence of a now extinct European Paleolithic dog population contributing to a genetically distinct dog population from either the Early or End Neolithic and therefore our results do not support the hypothesis of a large population replacement from East Asia during this era. Instead, we find that NGD is genetically very similar to HXH, both with ~75-80% of modern European-like ancestry as estimated with MixMapper and ADMIXTUREGRAPH. Additionally, CTC is most likely directly descended from a population represented by HXH, pointing to some genetic continuity throughout the Neolithic (over 2,000 years) in Central Europe. We find further support for this genetic continuity in the mtDNA phylogeny, which places all ancient samples, including an Upper Paleolithic, 12,500 year old German dog, together within sub-haplogroup C1 and as a sister clade of C1a and C1b.

However, the admixture events observed in European Neolithic dogs but not in most modern dogs (and even then to a lesser extent) from the same region suggest some degree of population structure on the continent during that period. This is further supported by HXH and NGD carrying both Southeast Asian ancestry but lacking the ancestry shared between CTC and modern Middle Eastern, Central and South Asian village dogs, even though NGD and CTC are contemporaneous (4,800 and 4,700 years old, respectively). It is likely that under this scenario of population structure, a different subpopulation eventually became dominant in modern European dogs, which may explain the observed mtDNA turnover from haplogroup C to A,

especially if this subpopulation also passed through a strong bottleneck. Additional support for population structure is the differential clustering of the ancient samples within C1 into a sub-haplogroup distinct from that of modern dogs. Though sample sizes are low, it is noteworthy that non-C haplogroups, including A, are more apparent in Southeast Europe in the archaeological record.

CTC shows similar admixture patterns to Central Asian and Middle Eastern modern dog populations, as seen in the PCA (Figure 2) and ADMIXTURE (Supplementary Figure S8.3.2.) analysis. Considering that the age of the samples provides a time frame, between 7,000 and 5,000 years ago, for CTC to obtain its unique ancestry component, and that the cranium was found next to two individuals associated with the Neolithic Corded Ware Culture, we speculate that this component was derived from incoming populations of dogs that accompanied steppe people migrating from the East. Moreover, ADMIXTUREGRAPH and *f4* statistics support the possibility that this ancestry and the wolf ancestry also detected in CTC are the consequence of the same admixture event, involving a dog population that carried both. This scenario is further supported by the model estimated by G-PhoCS, which infers substantial migration from wolves to the lineage represented by Indian village dogs, the modern population carrying the highest proportions of this ancestry.

As well as demonstrating a clear European component and genetic continuity with HXH, all analyses incorporating admixture in their model show a significant proportion of Indian-like ancestry in CTC (we note this component is predominant in some modern Indian dog populations but is also present in Central Asian and Middle Eastern dogs). However, in addition there is a potential wolf-like component observed from our NGSadmix and Spacemix analysis, as well as the Southeast Asian component that appears in all three Neolithic dogs. Given such a complex picture of admixture with four potential sources that must be inferred from a single genome, it is perhaps unsurprising that different methods r demonstrate somewhat wide variability in their inferred admixture proportions (from 25% in NGSadmix up to 69% in ADMIXTUREGRAPH). We hope that more genomes from Central Europe from this era will help clarify and better quantify this complicated picture of admixture in the future.

Our estimate of the “east-west” divergence time of ~17,500-23,900 years ago is compatible with that reported by Wang et al. [6] and Freedman et al.[31], but is considerably older than the time recently reported by Frantz et al. [11], when utilizing equivalent mutation rates. This split time is

consistent with the archeological record and can be explained without having to invoke a hypothesis of dual dog origins. The genomic continuity we see between our 7,000 year old HXH, the ~5,000 year old NGD and modern European samples implies that if there was any kind of population replacement, it must have occurred prior to the Neolithic (and perhaps much earlier given the matrilineal continuity between HXH, CTC and Bonn-Oberkassel). However, unlike the propositions of Frantz et al., such a replacement would necessarily be independent to the observed mtDNA turnover of C to A lineages, which does not appear to have occurred until at least 2,000 years after the end of the Neolithic (i.e. separated by at least 4,000 years).

We also estimated the dog-wolf divergence time to be 36,900-41,500 years (Figure 5b), which is consistent with predictions from the ancient Taimyr wolf genome [32]. Domestication must have occurred subsequent to the dog-wolf divergence and prior to Southeast Asian dog divergence (~17,500-23,900 years ago; Figure 5b). Altogether, our results provide an upper and lower bound for the onset of dog domestication, between ~20,000 and 40,000 years ago. However, whether this reflects a much older start for the dog domestication process than predicted by archaeological material (such as Bonn-Oberkassel) or a more recent descent of dogs from thus far unknown wolf populations remains an open question.

To date Southeast Asia, Europe, the Middle East and Central Asia have all been proposed as potential locations for the origin of dog domestication based on modern genomic data, archaeological evidence and ancient mitochondrial lineages[8,9,21,35]. While our analyses of three Neolithic genomes from Europe have helped narrow the timing of domestication, they are neither old enough nor do they have the broad geographic distribution necessary to resolve this debate. Nonetheless, our work does make clear that population structure and admixture have been a prominent feature of dog evolution for a substantial period of time. Population genetic analyses based only or primarily on modern data are unlikely to account for such complexity when modeling dog demographic history and, therefore, paleogenomic data from Upper Paleolithic remains throughout Eurasia will be crucial to ultimately resolve the location(s) of dog domestication.

Arising from numerous tandem duplication events, enhanced starch digestion through extreme *AMY2B* copy number expansion has been postulated to be an adaptation to the shift from the carnivorous diet of wolves to the starch-rich diet of domesticated dogs[37]. Although none of the German Neolithic samples carries the copy-number expansion of the *AMY2B* gene associated

with starch digestion, we find that this gene is present in three copies in NGD, though this is due to a large segmental duplication that is shared with multiple modern dogs, an event separate from the tandem *AMY2B* duplications. This suggests that the initial selection at this locus may have been independently driven by some factor other than *AMY2B* copy number. The absence of the extreme *AMY2B* copy number increase in these ancient samples indicates that the selective sweep associated with *AMY2B* expansion must have occurred well after the advent of agriculture and the Neolithic in Europe. This is consistent with recent findings that *AMY2B* copy number is bimodal, highest in modern dog populations originating from geographic regions with prehistoric agrarian societies, and lowest from regions where humans did not rely on agriculture for subsistence[40]. This supports the claim that the expansion occurred after initial domestication, and possibly after the migration of dingoes to Australia (3,500-5,000 years ago)[40]. A similar delayed pattern has been observed in humans, where alleles associated with lactase persistence in Europe rose to significant frequencies during the Bronze Age, i.e. 3,000 years after the introduction of pastoral livestock[25].

We report several discrepancies between our results and those from Frantz et al.[11] (PCA, divergence time estimates, AMY2B copy number, and ADMIXTUREGRAPH models). While results based on the SNP array data could be subject to biases due to the original variant ascertainment scheme (primarily based on European breed dogs), we replicated the results of all our analyses using SNPs identified from whole genome sequence data, which should be unbiased for the populations examined, suggesting robustness to the effects of ascertainment bias.

Overall, our findings reveal a history of domestic dogs as intricate as that of the people they lived alongside. The inference of complex patterns of gene flow is challenging, or even impossible, when only modern samples are studied. Therefore, the acquisition of a broader set of ancient samples, including ancient representatives from Central and Southeast Asia, and the Middle East will be crucial to further clarify the details of dog domestication and evolution.

Methods

Archaeological Background

HXH. A single petrous bone was identified in the internal ditch structure of Herxheim, an Early Neolithic site in Germany discovered in 1996, which contained archaeological material from the

Linearbandkeramik culture (LBK). Herxheim contains a significant amount of faunal remains, including >250 remains from dogs that constitute the largest bone series of Early Neolithic dogs in western Europe. A ^{14}C dating of 5223-5040 cal. BCE (95.4 %) was estimated for the bone (Mams-25941: 6186+/-30, calibrated with OxCal 4.2 [41] using the IntCal13 calibration curve [42]).

CTC. The entire cranium of a dog was found in the Kirschbaumhöhle (Cherry Tree Cave) in the Franconian Alb, Germany [15]. The cave was discovered in 2010 and contains human and animal remains from at least six prehistoric periods. CTC was an adult dog demonstrating morphological similarity to the so-called Torfhund (*Canis familiaris palustris*), and was found close to two human skulls dated to the early End Neolithic (2,800 - 2,600 cal. BCE). A ^{14}C dating of 2,900-2,632 cal. BCE (95.4 %) was estimated for the cranium (Erl-18378: 4194+/-45, calibrated with OxCal 4.2 using the IntCal13 calibration curve). See Supplementary Methods 1 for more details.

DNA Isolation and Screening

HXH. The petrous part of the temporal bone of sample HXH was prepared in clean-room facilities dedicated to ancient DNA in Trinity College Dublin (Ireland). DNA extraction was performed using a Silica column method as described in MacHugh et al. [43]. Two genomic libraries were prepared as described in Gamba et al. [44]. Screening of one library via an Illumina MiSeq run and mapping against various reference genomes demonstrated that reads for this sample mapped almost exclusively to the CanFam3 genome, revealing that it was a canid. Blank controls were utilized throughout. See Supplementary Methods 2 for more details.

CTC. Sample preparation was conducted in dedicated ancient DNA facilities of the Palaeogenetics Group at Johannes Gutenberg-University Mainz under strict rules for contamination prevention as described in Bramanti et al. [12]. DNA was extracted independently twice from the petrous bone using a phenol-chloroform protocol [45]. A total of four double indexed genomic libraries were prepared as described in Hofmanová et al. [13]. One library was screened for endogenous DNA content via Illumina MiSeq sequencing, with 61.5% of reads mapping to CanFam3. Blank controls were utilized throughout. See Supplementary Methods 3 for more details.

Genome sequencing and Bioinformatic Processing

Combinations of various genomic libraries from each ancient sample (CTC and HXH) were sequenced on two lanes of an Illumina HiSeq 2500 1TB at the New York Genome Center (NYGC) using the High Output Run mode to produce 2x125bp paired-end reads. Reads were trimmed, merged and filtered using a modified version of the ancient DNA protocol described by Kircher [46]. Merged reads were then mapped using `BWA aln` [47] to a modified version of the CanFam3.1 reference genome containing a Y chromosome. Duplicate reads were identified and marked using `PICARD MarkDuplicates`, resulting in a mean coverage for both samples of 9x. Additionally, the mean coverage for the X and Y chromosomes was ~5x for both samples, indicating they were males. Mean fragment length for both samples ranged from 60-70bp. Post-mortem degradation effects were assessed using `MapDamage_v1.0` [16], revealing extensive 5' C>T and 3' G>A damage. Single-ended reads for NGD extracted from a `BAM` file containing all mapped reads were processed using the same pipeline. See Supplementary Methods 4 for more details.

Genotype likelihood estimation and genotype calling for all three ancient samples was performed using a custom caller that takes into account post-mortem damage patterns identified by `MapDamage` based on the model described in Hofmanová et al. [13]. Briefly, damage patterns with respect to read position are fit with a Weibull distribution of the form a X exp(-(x^c) X b), where x is the proportion of damaged C>T or G>A bases at a particular position along the read (unlike Hofmanová et al. [13], we find a slightly better fit with a Weibull than when assuming exponential decay (Supplementary Figure S5.1.1). Any site with less than 7x coverage was reported as missing. In addition, any position where the highest likelihood is a heterozygote must have a minimum Phred-scaled genotype quality of 30 or the next highest homozygote likelihood genotype was chosen instead. The code is available at https://github.com/kveeramah/aDNA_GenoCaller. This protocol substantially decreased the overrepresentation of C>T and G>A sites identified by `GATK UnifiedGenotyper` [48], which does not account for post-mortem damage. See Supplementary Methods 5 for more details. Additionally, base calls with a quality score less than 15 and reads with a mapping quality less than 15 were not included during genotype calling. Base calls with a quality score greater than 40 (which can occur during paired-end read merging) were adjusted to 40.

Reference Dataset

Genome Sequence Data. In addition to the three ancient samples, we examined whole genome sequence data from 96 modern canids. Additional genomes were generated using Illumina

sequencing for a Great Dane and Iberian wolf (SRP073312). We also posted sequencing reads to the SRA for a Portuguese village dog, Chinese Mongolian Shepherd village dog and a Sub-Saharan African village dog (SRP034749). All remaining genome data were acquired from previously published datasets deposited on SRA. As above, reads for all modern canids were aligned to CanFam3.1 using BWA, followed by GATK quality score recalibration, and genotype calling using HaplotypeCaller [48]. These data were supplemented with genotype data for six canids from Freedman et al. [31] (basenji, dingo, golden jackal, Croatian wolf, Israeli wolf, and Chinese wolf). We generated three different call sets with different ascertainment schemes. Call set 1 includes all variants from both ancient and contemporary genomes, representing the most comprehensive set of variants, but may show biases due to differences in coverage among sample sets. Call set 2 only includes variants discovered in the three ancient genomes. Call set 3 only includes sites discovered as variable in New World wolves, and is the primary call set utilized for most analyses. See Supplementary Methods 6 for more details.

SNP array data. Canine SNP array datasets were obtained from Shannon et al. [8] and Pilot et al. [18]. Genotypes were also supplemented by data from the six canids reported in Freedman et al. [31].

Statistical Analysis

mtDNA. The average sequencing depth for mtDNA was 179x, 208x and 170x in the CTC, HXH and NGD samples, respectively. Ancient sample mtDNA consensus sequences were aligned to the canid alignment from Thalmann et al. [9], which contain whole mtDNA genomes for both modern and ancient canids. A NJ tree was built with a TN93 substitution model (500 bootstraps) using MEGA 6.06 [49]. A further NJ tree was built with additional C1 and C2 samples from Duleba et al. [22]. See Supplementary Methods 7 for more details.

Population Structure. Principle component analysis was performed on both the SNP array dataset and genome SNP Call set 3 using smartpca, part of the EIGENSOFT package version 3.0 [50]. Both diploid and pseudo-haploid genotype calls with and without C<>T and G<>A SNPs (the most likely sites to undergo post-mortem damage) were used to construct the PCA, but little difference was found amongst these analyses. SpaceMix [29] was used to create a geogenetic map and infer potential long-distance admixture events across this map using the SNP array data, allowing only SNPs separated by at least 100kb and no more than five individuals per population. Multiple runs were performed with 10 initial burn-ins of 100,000 generations and a

final long run of 10,000,000 generations. ADMIXTURE (v. 1.22) [51] was used to perform an unsupervised clustering analysis on the SNP array data for the ancient dogs and a subset of 105 modern dogs that provided a global representation of dog structure, while NGSadmix [52] was used to perform a similar analysis for the genome SNP data while taking into account genotype uncertainty by examining genotype likelihoods. Cross validation was performed for the ADMIXTURE analysis to identify the most appropriate number of clusters, *K*. See Supplementary Methods 8 for more details.

Neighbor-Joining tree construction. NJ trees were constructed for the whole genome SNP set using the ape R package [53] using distance matrices based on the metric of sequence divergence from Gronau et al. [30]. One hundred bootstrap replicates were generated by dividing the genome into 5 cM windows and sampling with replacement in order to determine node support. See Supplementary Methods 9 for more details.

F and D-statistics-based analysis. Outgroup-*f3* statistics to assess relative genetic drift between ancient and modern dogs, *D*-statistics to identify potential ancient dog-wolf admixture and *f4*-ratio tests to estimate dog-dog and dog-wolf admixture proportions were calculated using Admixtools [28]. Both MixMapper [27] and ADMIXTUREGRAPH [28] were used to perform model-based inference of specific admixture events involving the three ancient dogs. MixMapper was performed on both the SNP array and whole genome SNP datasets, whereas ADMIXTUREGRAPH was performed on the whole genome dataset only. Significance was assessed using a weighted block jackknife procedure for all five analysis types. Genetic map positions for each SNP used in these analyses were inferred from Auton et al. [54]. See Supplementary Methods 11 and 12 for more details.

G-PhoCS and HXH divergence estimation. G-PhoCS [30] was used to estimate divergence times, effective population sizes and migration rates for various modern dog and wolf combinations using sequence alignments from 16,434 “neutral” loci previously identified in Freedman et al. [31] after LiftOver from CanFam3 to CanFam3.1. NJ trees were constructed to inform the topology of population divergence. 500,000 MCMC iterations were found to be sufficient for convergence for our data, with the last 200,000 used to estimate posterior distributions. We then developed a numerical approach based on coalescent theory to predict the ratio of shared derived sites between HXH/NGD and European village dogs versus Indian and European

village dogs given the parameters estimated by G-PhoCS for European, Indian and Southeast Asian population divergence and a particular divergence time of HXH/NGD in units of expected numbers of mutations. Confidence intervals were estimated by resampling G-PhoCS parameters from their posterior distributions and finding predicted derived allele sharing ratios that were within a range determined for the observed data by a weighted jackknife resampling approach. See Supplementary Methods 11 and 12 for more details.

Genotyping at loci associated with the domestication process. Coordinates of thirty putative "domestication loci" were obtained from Axelsson et al. [37] and lifted over from CanFam2.0 to CanFam3.1 coordinates. Call set 1 SNPs within each window were extracted from the ancient samples and our genome sequence dataset. Eigenstrat genotype file formats were generated per window using convertf from the EIGENSOFT package [55] and custom scripts were used to convert the genotype files into matrix formats for visualization using matrix2png [56] using a filtered subset of SNPs (minor allele frequencies between 0.05 and 0.49) for easing visualization of the matrices. NJ trees were estimated for each window with the full SNP set using the same methods as the whole genome tree estimation (see above). Altogether, the haplotypes of the three ancient samples were classified as either dog or wolf-like for 18 matrices that showed clear distinction between dog and wild canid haplotypes based on average reference allele counts calculated per window. See Supplementary Methods 14 for more details.

Copy-number variation at the amylase 2B locus. Genomic copy-number was estimated from read depth as previously described [57,58]. Reads were split into non-overlapping 36bp fragments and mapped to a repeat-masked version of the CanFam3.1 reference using mrsFAST [59], returning all read placements with two or fewer substitutions. Raw read depths were tabulated at each position and a loess correction for local GC content was calculated utilizing control regions not previously identified as copy number variable. The mean depth in 3kb windows was then calculated and converted to estimated copy-number based on the depth in the autosomal control regions. See Supplementary Methods 14 for more details.

Data Access

Sequencing data is available from the NCBI sequence read archive (SRA) database under accession numbers SRS1407451 (CTC) and SRS1407453 (HXH), and mitochondrial genomes are available in GenBank under accessions KX379528 and KX379529, respectively.

Code generated to call variants in the ancient samples is available at:
https://github.com/kveeramah/aDNA_GenoCaller

References

1. Parker, H. G. *et al.* Genetic structure of the purebred domestic dog. *Science* **304,** 1160–1164 (2004).
2. Benecke, N. Studies on early dog remains from Northern Europe. *J. Archaeol. Sci.* **14,** 31–49 (1987).
3. Perri, A. A wolf in dog's clothing: Initial dog domestication and Pleistocene wolf variation. *J. Archaeol. Sci.* **68,** 1–4 (2016).
4. Horard-Herbin, M.-P., Tresset, A. & Vigne, J.-D. Domestication and uses of the dog in western Europe from the Paleolithic to the Iron Age. *Animal Frontiers* **4,** 23–31 (2014).
5. Savolainen, P., Zhang, Y.-P., Luo, J., Lundeberg, J. & Leitner, T. Genetic evidence for an East Asian origin of domestic dogs. *Science* **298,** 1610–1613 (2002).
6. Wang, G.-D. *et al.* Out of southern East Asia: the natural history of domestic dogs across the world. *Cell Res.* **26,** 21–33 (2016).
7. Vonholdt, B. M. *et al.* Genome-wide SNP and haplotype analyses reveal a rich history underlying dog domestication. *Nature* **464,** 898–902 (2010).
8. Shannon, L. M. *et al.* Genetic structure in village dogs reveals a Central Asian domestication origin. *Proc. Natl. Acad. Sci. U. S. A.* **112,** 13639–13644 (2015).
9. Thalmann, O. *et al.* Complete mitochondrial genomes of ancient canids suggest a European origin of domestic dogs. *Science* **342,** 871–874 (2013).
10. Deguilloux, M. F., Moquel, J., Pemonge, M. H. & Colombeau, G. Ancient DNA supports lineage replacement in European dog gene pool: insight into Neolithic southeast France. *J. Archaeol. Sci.* **36,** 513–519 (2009).
11. Frantz, L. A. F. *et al.* Genomic and archaeological evidence suggest a dual origin of domestic dogs. *Science* **352,** 1228–1231 (2016).
12. Bramanti, B. *et al.* Genetic discontinuity between local hunter-gatherers and central

Europe's first farmers. *Science* **326,** 137–140 (2009).

13. Hofmanová, Z. *et al.* Early farmers from across Europe directly descended from Neolithic Aegeans. *Proc. Natl. Acad. Sci. U. S. A.* (2016). doi:10.1073/pnas.1523951113
14. Haak, W. *et al.* Massive migration from the steppe was a source for Indo-European languages in Europe. *Nature* **522,** 207–211 (2015).
15. Seregély, T., Burgdorf, P., Gresik, G., Müller, M. S. & Wilk, A. „Tote Menschen und Tiere in finsteren Felsschächten…"-neue Dokumentationsmethodik und erste Untersuchungsergebnisse zur Kirschbaumhöhle in Oberfranken. *Praehistorische Zeitschrift* **90,** 214–244 (2015).
16. Ginolhac, A., Rasmussen, M., Gilbert, M. T. P., Willerslev, E. & Orlando, L. mapDamage: testing for damage patterns in ancient DNA sequences. *Bioinformatics* **27,** 2153–2155 (2011).
17. Briggs, A. W. *et al.* Patterns of damage in genomic DNA sequences from a Neandertal. *Proc. Natl. Acad. Sci. U. S. A.* **104,** 14616–14621 (2007).
18. Pilot, M. *et al.* On the origin of mongrels: evolutionary history of free-breeding dogs in Eurasia. *Proc. Biol. Sci.* **282,** 20152189 (2015).
19. Patterson, N. *et al.* Ancient admixture in human history. *Genetics* **192,** 1065–1093 (2012).
20. Fan, Z. *et al.* Worldwide patterns of genomic variation and admixture in gray wolves. *Genome Res.* **26,** 163–173 (2016).
21. Anderson, T. M. *et al.* Molecular and evolutionary history of melanism in North American gray wolves. *Science* **323,** 1339–1343 (2009).
22. Duleba, A., Skonieczna, K., Bogdanowicz, W., Malyarchuk, B. & Grzybowski, T. Complete mitochondrial genome database and standardized classification system for Canis lupus familiaris. *Forensic Sci. Int. Genet.* **19,** 123–129 (2015).
23. Larson, G. *et al.* Rethinking dog domestication by integrating genetics, archeology, and biogeography. *Proc. Natl. Acad. Sci. U. S. A.* **109,** 8878–8883 (2012).

24. Rasmussen, M. *et al.* The genome of a Late Pleistocene human from a Clovis burial site in western Montana. *Nature* **506,** 225–229 (2014).

25. Allentoft, M. E. *et al.* Population genomics of Bronze Age Eurasia. *Nature* **522,** 167–172 (2015).

26. Jones, E. R. *et al.* Upper Palaeolithic genomes reveal deep roots of modern Eurasians. *Nat. Commun.* **6,** 8912 (2015).

27. Lipson, M. *et al.* Efficient Moment-Based Inference of Admixture Parameters and Sources of Gene Flow. *Mol. Biol. Evol.* **30,** 1788–1802 (2013).

28. Patterson, N. *et al.* Ancient admixture in human history. *Genetics* **192,** 1065–1093 (2012).

29. Bradburd, G., Ralph, P. L. & Coop, G. *A Spatial Framework for Understanding Population Structure and Admixture*. (2015). doi:10.1101/013474

30. Gronau, I., Hubisz, M. J., Gulko, B., Danko, C. G. & Siepel, A. Bayesian inference of ancient human demography from individual genome sequences. *Nat. Genet.* **43,** 1031–1034 (2011).

31. Freedman, A. H. *et al.* Genome sequencing highlights the dynamic early history of dogs. *PLoS Genet.* **10,** e1004016 (2014).

32. Skoglund, P., Ersmark, E., Palkopoulou, E. & Dalén, L. Ancient wolf genome reveals an early divergence of domestic dog ancestors and admixture into high-latitude breeds. *Curr. Biol.* **25,** 1515–1519 (2015).

33. Wang, G.-D. *et al.* The genomics of selection in dogs and the parallel evolution between dogs and humans. *Nat. Commun.* **4,** 1860 (2013).

34. Kumar, S. & Subramanian, S. Mutation rates in mammalian genomes. *Proc. Natl. Acad. Sci. U. S. A.* **99,** 803–808 (2002).

35. Wang, G.-D. *et al.* Out of southern East Asia: the natural history of domestic dogs across the world. *Cell Res.* **26,** 21–33 (2016).

36. Song, S., Sliwerska, E., Emery, S. & Kidd, J. M. Modeling Human Population Separation

History Using Physically Phased Genomes. *Genetics* **205,** 385–395 (2017).

37. Axelsson, E. *et al.* The genomic signature of dog domestication reveals adaptation to a starch-rich diet. *Nature* **495,** 360–364 (2013).
38. Arendt, M., Fall, T., Lindblad-Toh, K. & Axelsson, E. Amylase activity is associated with AMY2B copy numbers in dog: implications for dog domestication, diet and diabetes. *Anim. Genet.* **45,** 716–722 (2014).
39. Reiter, T., Jagoda, E. & Capellini, T. D. Dietary Variation and Evolution of Gene Copy Number among Dog Breeds. *PLoS One* **11,** e0148899 (2016).
40. Arendt, M., Cairns, K. M., Ballard, J. W. O., Savolainen, P. & Axelsson, E. Diet adaptation in dog reflects spread of prehistoric agriculture. *Heredity* (2016). doi:10.1038/hdy.2016.48
41. Ramsey, C. B. Bayesian analysis of radiocarbon dates. *Radiocarbon* **51,** 337–360 (2009).
42. Reimer, P. J. *et al.* IntCal13 and Marine13 Radiocarbon Age Calibration Curves 0–50,000 Years cal BP. *Radiocarbon* **55,** 1869–1887 (2013).
43. MacHugh, D. E., Edwards, C. J., Bailey, J. F., Bancroft, D. R. & Bradley, D. G. The extraction and analysis of ancient DNA from bone and teeth: a survey of current methodologies. *Anc. Biomol.* **3,** 81–102 (2000).
44. Gamba, C. *et al.* Genome flux and stasis in a five millennium transect of European prehistory. *Nat. Commun.* **5,** 5257 (2014).
45. Scheu, A. *et al.* The genetic prehistory of domesticated cattle from their origin to the spread across Europe. *BMC Genet.* **16,** 54 (2015).
46. Kircher, M. Analysis of high-throughput ancient DNA sequencing data. *Methods Mol. Biol.* **840,** 197–228 (2012).
47. Li, H. & Durbin, R. Fast and accurate long-read alignment with Burrows-Wheeler transform. *Bioinformatics* **26,** 589–595 (2010).
48. DePristo, M. A. *et al.* A framework for variation discovery and genotyping using next-generation DNA sequencing data. *Nat. Genet.* **43,** 491–498 (2011).

49. Tamura, K., Stecher, G., Peterson, D., Filipski, A. & Kumar, S. MEGA6: Molecular Evolutionary Genetics Analysis version 6.0. *Mol. Biol. Evol.* **30,** 2725–2729 (2013).

50. Patterson, N., Price, A. L. & Reich, D. Population structure and eigenanalysis. *PLoS Genet.* **2,** e190 (2006).

51. Alexander, D. H., Novembre, J. & Lange, K. Fast model-based estimation of ancestry in unrelated individuals. *Genome Res.* **19,** 1655–1664 (2009).

52. Skotte, L., Korneliussen, T. S. & Albrechtsen, A. Estimating individual admixture proportions from next generation sequencing data. *Genetics* **195,** 693–702 (2013).

53. Paradis, E., Claude, J. & Strimmer, K. APE: Analyses of Phylogenetics and Evolution in R language. *Bioinformatics* **20,** 289–290 (2004).

54. Auton, A. *et al.* Genetic recombination is targeted towards gene promoter regions in dogs. *PLoS Genet.* **9,** e1003984 (2013).

55. Price, A. L. *et al.* Principal components analysis corrects for stratification in genome-wide association studies. *Nat. Genet.* **38,** 904–909 (2006).

56. Pavlidis, P. & Noble, W. S. Matrix2png: a utility for visualizing matrix data. *Bioinformatics* **19,** 295–296 (2003).

57. Sudmant, P. H. *et al.* Diversity of human copy number variation and multicopy genes. *Science* **330,** 641–646 (2010).

58. Alkan, C. *et al.* Personalized copy number and segmental duplication maps using next-generation sequencing. *Nat. Genet.* **41,** 1061–1067 (2009).

59. Hach, F. *et al.* mrsFAST: a cache-oblivious algorithm for short-read mapping. *Nat. Methods* **7,** 576–577 (2010).

Acknowledgements

We thank Dan Bradley for his help obtaining the HXH specimen. We thank Walter Eanes and Douglas Futuyma for their comments on the manuscript, Dorina Twigg for the processing of canine copy-number variation data, Nick Patterson for providing advanced access to the latest version of `Admixtools`, Vida for his thoughts, the NYGC for their assistance in the sequencing, Valeria Mattiangeli for performing initial Miseq sequencing on HXH, Christian Sell for his assistance with the raw data analysis pipeline used for the CTC Miseq data, and the Musée zoologique de la Ville de Strasbourg for hosting the team of archaezoology. The Kidd Lab is supported by grant R01GM103961 and Amanda Pendleton is supported by T32HG00040. Amelie Scheu and Kevin Daly are supported by the EU: CodeX Project No: 295729. Laura Botigué is supported by the Beatriu de Pinós Fellowship, from Generalitat de Catalunya. Shyamalika Gopalan was supported by a Boehringer Ingelheim Fonds Travel award.

Author contributions

T.S, A.Z and R.A provided the archaeological material. A.S, S.G, K.D and M.U performed the ancient DNA lab work and screening. L.R.B, S.S, A.L.P, M.O, A.M.T, D.B, J.M.K and K.R.V performed the downstream bioinformatics and population genetic analysis. L.R.B, J.B and K.R.V conceived the study. L.R.B and K.R.V wrote the paper.

Disclosure Declaration

All authors declare no financial interests

Figure Legends

Figure 1. Phylogeny of ancient and contemporary canids. a) Phylogeny based on mtDNA. Age of the samples is indicated in parentheses, wolf samples are shown in orange. **b)** Neighbor-joining tree based on pairwise sequence divergence from whole genome data.

Figure 2. PCA between ancient and contemporary canids. a) PCA of village dogs, with breed dogs and ancient dogs projected onto the PC space using SNP array data. **b)** PCA of village dogs, breed dogs and ancient dogs using whole genome SNP data ascertained in the New World wolves.

Figure 3. Genetic affinity of ancient samples. Heat map of outgroup $f3$-statistics of the form $f3$ (golden jackal; ancient sample; X) based on SNP array genotype data. Higher $f3$ values indicate increased shared drift between the samples, and therefore higher genetic similarities. **a)** HXH shows greatest similarity with NGD and modern European village dogs (higher $f3$ values), and is most distant to East Asian and Indian village dogs. **b)** CTC shares the most genetic similarity with HXH, followed by NGD and other European

dogs. In addition, CTC shows greater similarity to village dogs from India (particularly unadmixed populations in the east) than HXH does.

Figure 4 Population structure between ancient and contemporary canids. NGSadmix clustering for K=4 for village dogs, ancient dogs and Old World wolves based on the whole genome SNP data.

Figure 5 Demographic model regarding ancient and contemporary dogs and wolves. a) The best model fit to both modern and ancient canid data using ADMIXTUREGRAPH on the whole genome dataset. This model had four *f4-statistic* outliers. Branches are indicated by solid black lines (adjacent numbers indicate estimated drift values in units of *f2* distance, parts per thousand), whereas admixture is indicated by coloured dashed lines (adjacent numbers indicate ancestry proportions). Sampled individuals/populations are indicated by solid circles with bold outline. Wolves are labeled as "wolf" and dogs are labeled according to their continental origin. **b)** Divergence times of contemporary dogs and wolves inferred using G-PhoCS. Mean estimates are indicated by squares with ranges correspond to 95% Bayesian credible intervals. Migration bands are shown in grey with associated value representing the inferred total migration rates (the probability that a lineage in the target population will migrate into the source population). The divergence time for HXH and NGD and modern European dogs is inferred using a numerical approach. The proportion of Indian village dog ancestry in CTC are inferred by NGSadmix and the proportion of South China village dog ancestry in HXH and NGD are inferred by *f4* ratio test, shown in red.

Figure 6. Haplotype and copy-number variation at the amylase 2B (*AMY2B*) locus. a) Genotype matrix of selected sites within F_{ST}-derived domestication locus 12 (chr6: 46854109-47454177)[37]. SNP genotypes are represented as either homozygous for the reference allele (0/0; blue), heterozygous (0/1; white), or homozygous (1/1; orange) for the alternate allele. The positions of *AMY2B* (green line) and *RNPC3* (model above) are indicated. **b)** Read-depth based estimation of *AMY2B* copy number for the Andean fox (light green), golden jackal (light green), coyotes (dark green), wolves (orange), ancient samples (red), village dogs (purple), and breed dogs (blue). Dashed line indicates diploid copy number of two.

Figure 1

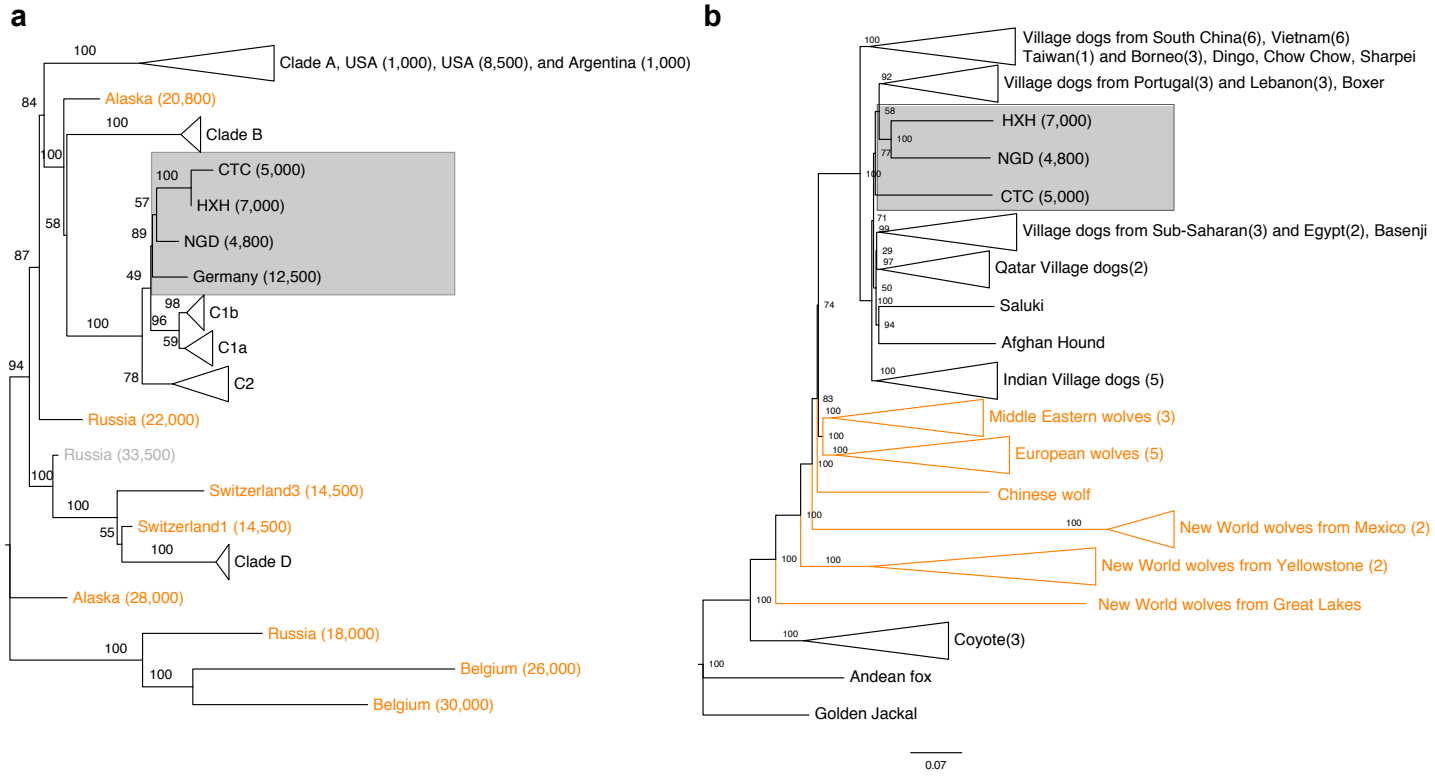
a
Clade A, USA (1,000), USA (8,500), and Argentina (1,000)
Alaska (20,800)
Clade B
CTC (5,000)
HXH (7,000)
NGD (4,800)
Germany (12,500)
C1b
C1a
C2
Russia (22,000)
Russia (33,500)
Switzerland3 (14,500)
Switzerland1 (14,500)
Clade D
Alaska (28,000)
Russia (18,000)
Belgium (26,000)
Belgium (30,000)
b
Village dogs from South China(6), Vietnam(6)
Taiwan(1) and Borneo(3), Dingo, Chow Chow, Sharpei
Village dogs from Portugal(3) and Lebanon(3), Boxer
HXH (7,000)
NGD (4,800)
CTC (5,000)
Village dogs from Sub-Saharan(3) and Egypt(2), Basenji
Qatar Village dogs(2)
Saluki
Afghan Hound
Indian Village dogs (5)
Middle Eastern wolves (3)
European wolves (5)
Chinese wolf
New World wolves from Mexico (2)
New World wolves from Yellowstone (2)
New World wolves from Great Lakes
Coyote(3)
Andean fox
Golden Jackal
0.07

Figure 2

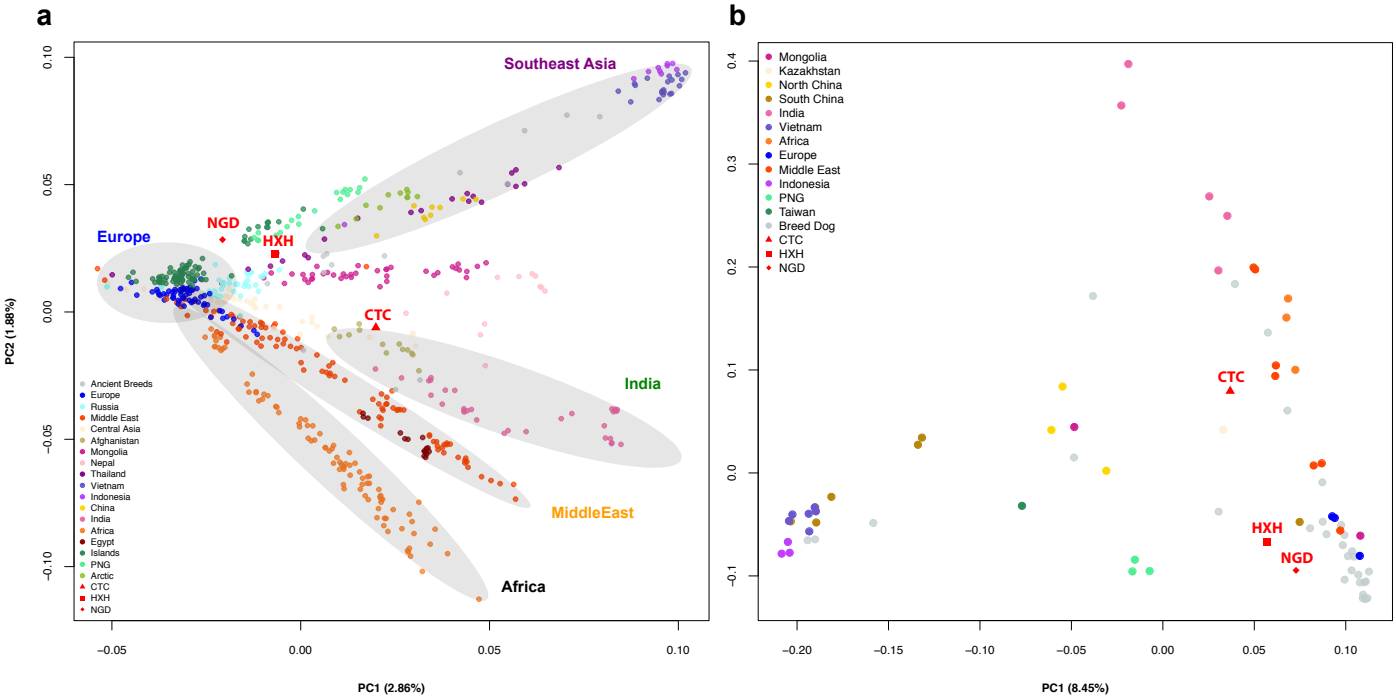
a
Southeast Asia
Europe
NGD
HXH
CTC
India
MiddleEast
Africa
Ancient Breeds
Europe
Russia
Middle East
Central Asia
Afghanistan
Mongolia
Nepal
Thailand
Vietnam
Indonesia
China
India
Africa
Egypt
Islands
PNG
Arctic
CTC
HXH
NGD
PC2 (1.88%)
PC1 (2.86%)
b
Mongolia
Kazakhstan
North China
South China
India
Vietnam
Africa
Europe
Middle East
Indonesia
PNG
Taiwan
Breed Dog
CTC
HXH
NGD
PC1 (8.45%)

Figure 3

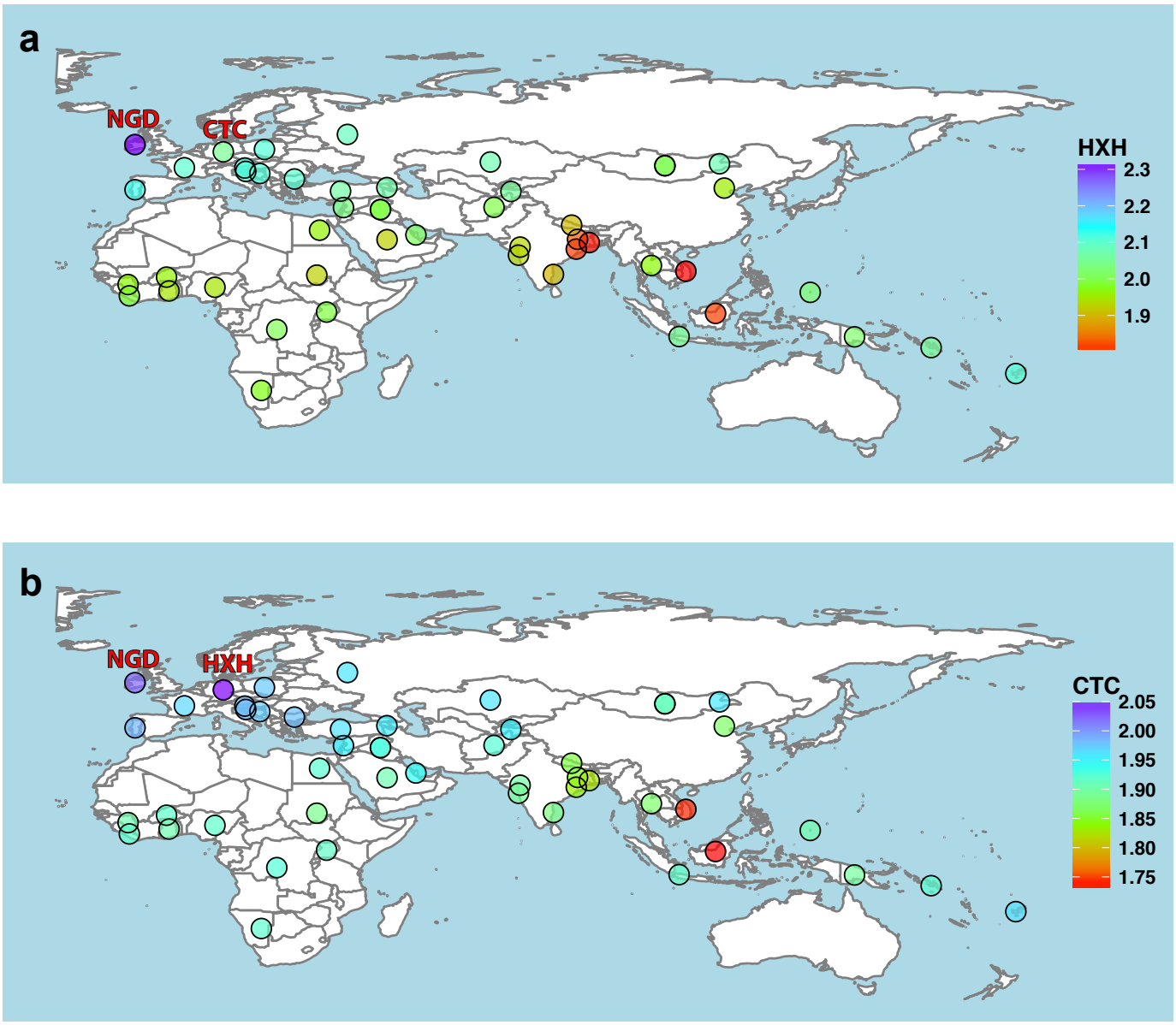
a
NGD
CTC
HXH
2.3
2.2
2.1
2.0
1.9
b
NGD
HXH
CTC
2.05
2.00
1.95
1.90
1.85
1.80
1.75

Figure 4

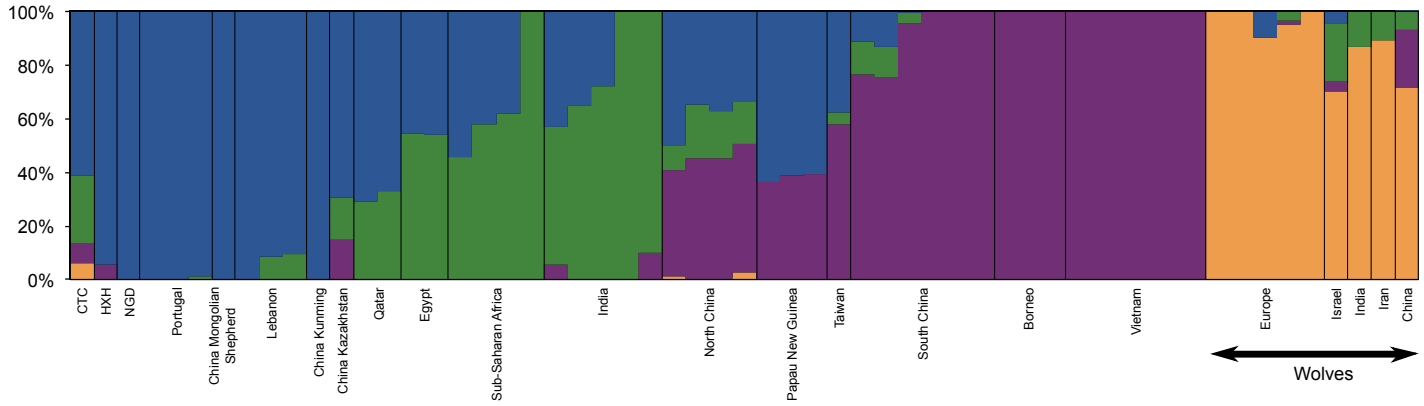
100%
80%
60%
40%
20%
0%
CTC
HXH
NGD
Portugal
China Mongolian Shepherd
Lebanon
China Kunming
China Kazakhstan
Qatar
Egypt
Sub-Saharan Africa
India
North China
Papau New Guinea
Taiwan
South China
Borneo
Vietnam
Europe
Israel
India
Iran
China
Wolves

Figure 5

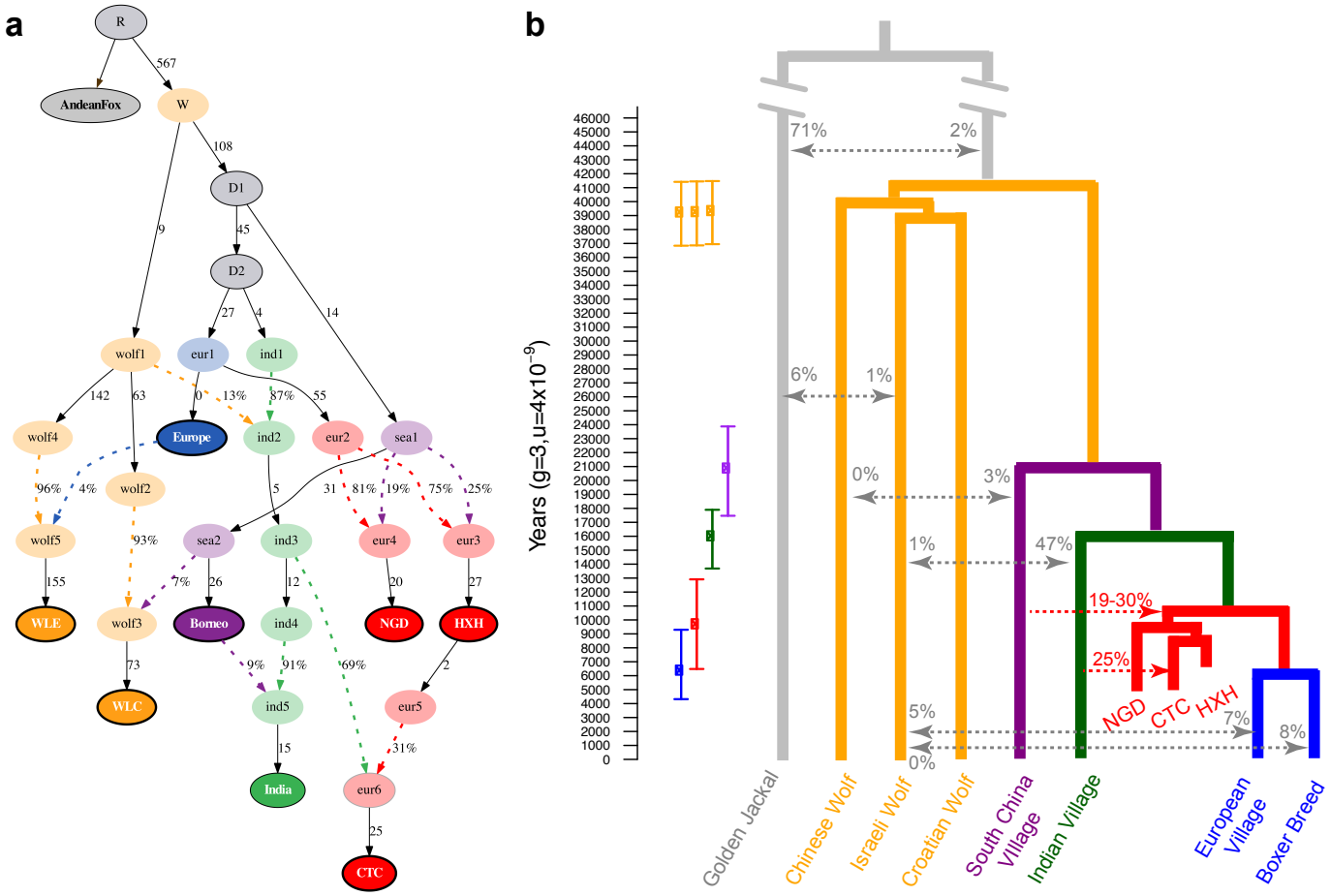
a
R
567
AndeanFox
W
108
D1
9
45
D2
27
4
14
wolf1
eur1
ind1
142
63
0
13%
87%
55
wolf4
Europe
ind2
eur2
sea1
96%
4%
wolf2
5
31
81%
19%
75%
25%
wolf5
93%
sea2
ind3
eur4
eur3
155
7%
26
12
20
27
WLE
wolf3
Borneo
ind4
NGD
HXH
73
9%
91%
69%
2
WLC
ind5
eur5
15
31%
India
eur6
25
CTC
b
Years (g=3,u=4x10^{-9})
46000
45000
44000
43000
42000
41000
40000
39000
38000
37000
36000
35000
34000
33000
32000
31000
30000
29000
28000
27000
26000
25000
24000
23000
22000
21000
20000
19000
18000
17000
16000
15000
14000
13000
12000
11000
10000
9000
8000
7000
6000
5000
4000
3000
2000
1000
0
71%
2%
6%
1%
0%
3%
1%
47%
19-30%
25%
5%
0%
7%
8%
NGD
CTC
HXH
Golden Jackal
Chinese Wolf
Israeli Wolf
Croatian Wolf
South China Village
Indian Village
European Village
Boxer Breed

Figure 6

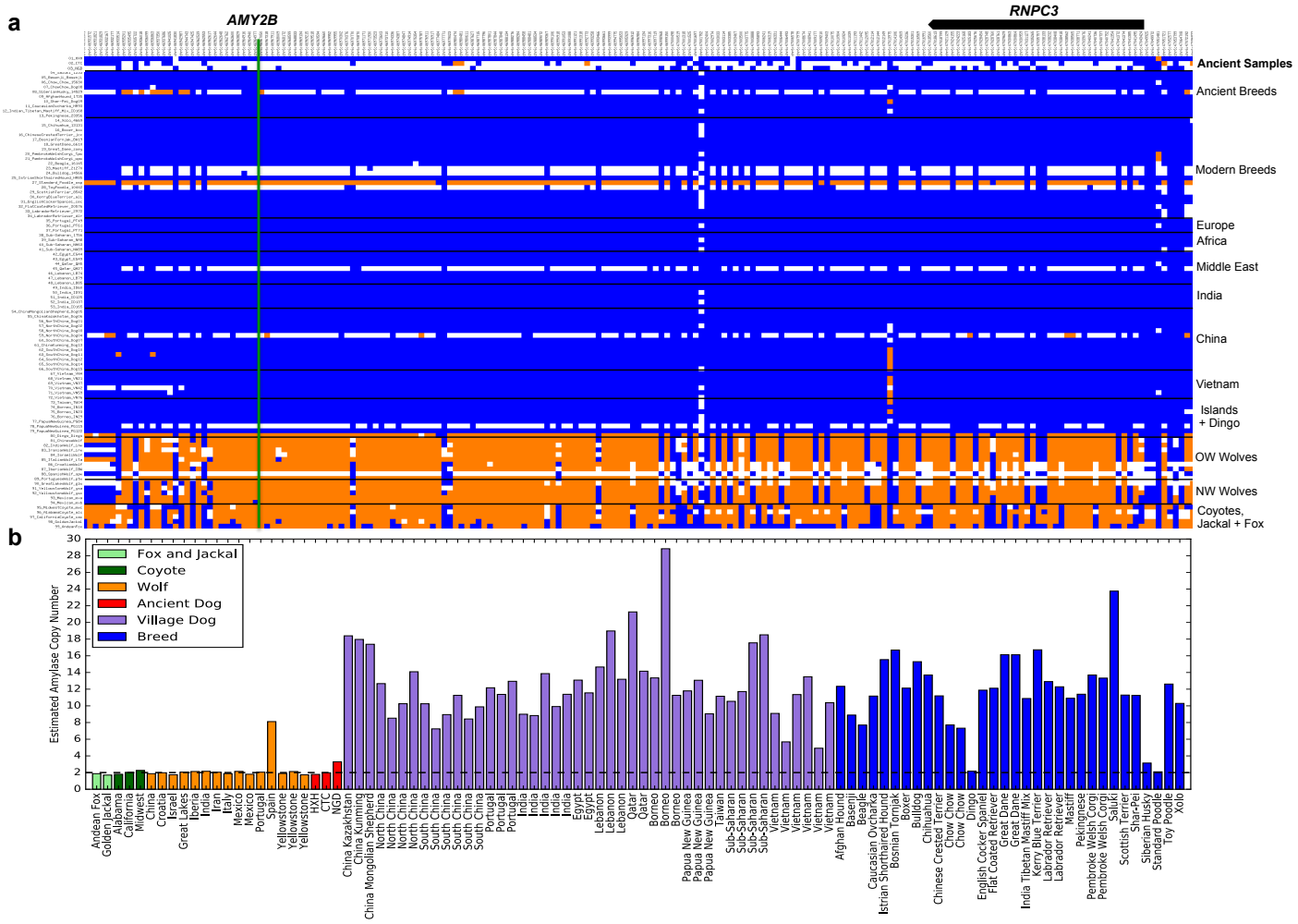
a
AMY2B
RNPC3
Ancient Samples
Ancient Breeds
Modern Breeds
Europe
Africa
Middle East
India
China
Vietnam
Islands
+ Dingo
OW Wolves
NW Wolves
Coyotes,
Jackal + Fox
b
Fox and Jackal
Coyote
Wolf
Ancient Dog
Village Dog
Breed
Estimated Amylase Copy Number
0
2
4
6
8
10
12
14
16
18
20
22
24
26
28
30
Andean Fox
Golden Jackal
Alabama
California
Midwest
China
Croatia
Israel
Great Lakes
Iberia
India
Iran
Italy
Mexico
Mexico
Portugal
Spain
Yellowstone
Yellowstone
Yellowstone
HXH
CTC
NGD
China Kazakhstan
China
China Kunming
China Mongolian Shepherd
North China
North China
North China
North China
South China
South China
South China
South China
South China
South China
South China
Portugal
Portugal
Portugal
India
India
India
India
India
India
Egypt
Egypt
Lebanon
Lebanon
Lebanon
Qatar
Qatar
Borneo
Borneo
Borneo
Borneo
Papua New Guinea
Papua New Guinea
Papua New Guinea
Taiwan
Sub-Saharan
Sub-Saharan
Sub-Saharan
Sub-Saharan
Vietnam
Vietnam
Vietnam
Vietnam
Vietnam
Vietnam
Vietnam
Afghan Hound
Basenji
Beagle
Caucasian Ovcharka
Istrian Shorthaired Hound
Bosnian Tornjak
Boxer
Bulldog
Chihuahua
Chinese Crested Terrier
Chow Chow
Chow Chow
Dingo
English Cocker Spaniel
Flat Coated Retriever
Great Dane
Great Dane
India Tibetan Mastiff Mix
Kerry Blue Terrier
Labrador Retriever
Labrador Retriever
Mastiff
Pekingnese
Pembroke Welsh Corgi
Pembroke Welsh Corgi
Saluki
Scottish Terrier
Shar-Pei
Siberian Husky
Standard Poodle
Toy Poodle
Xolo